A Combined Experimental and Theoretical Study of the Homogeneous, Unimolecular Decomposition Kinetics of 3-Chloropivalic Acid in the Gas Phase

Gabriel Chuchani,[†] Alexandra Rotinov,[†] Juan Andrés,*[,‡] Luís R. Domingo,[§] and V. Sixte Safont[‡]

Centro de Química, Instituto Venezolano de Investigaciones Científicas (I.V.I.C.), Box 21827, Caracas 1020-A, Venezuela, Departament de Ciències Experimentals, Universitat Jaume I, Box 224, 12080 Castelló, Spain, and Departament de Química Orgànica, Universitat de València, Dr. Moliner 50, 46100 Burjassot, València, Spain

Received: September 29, 2000; In Final Form: December 7, 2000

Decomposition kinetics of 3-chloropivalic acid in the gas phase were determined in a static system over the temperature and pressure ranges of 380.5−430.1 °C and 43−120 Torr, respectively. The reaction, in vessel seasoned with allyl bromide, and in the presence of free-radical suppresser toluene, is homogeneous, unimolecular, and follows a first-order rate law. The rate coefficients are given by the following equation: $\log k_1\ (s^{-1}) = (12.42 \pm 0.36) - (205.8 \pm 4.7)$ kJ mol^{-1} $(2.303RT)^{-1}$. The reaction mechanism for the formation of isobutene, hydrogen chloride, and carbon dioxide has been theoretically characterized. The theoretical study, at MP2/6-31G** computational level, points out that the molecular mechanism corresponds to a concerted and highly synchronous process yielding the products. An analysis of bond orders and NBO charges shows that the polarization of the C−Cl breaking bond can be considered the driving force for this fragmentation process. The rate coefficients obtained from experimental data and theoretical calculations are in good agreement.

1. Introduction

Kinetic studies on the decomposition of different 2-substituted carboxylic acid derivatives have been carried out by some of us.[1−5] The results show that the reaction is homogeneous, unimolecular and obeys a first-order rate law. Two different molecular mechanisms have been proposed: (i) a hydrogen chloride elimination, and (ii) a pathway conducted by the neighboring group participation of the carbonyl oxygen of the COOH group coupled with the C−Cl bond polarization (Scheme 1). Both proposals take place along a two-step mechanism: the first step is the formation of the α-lactone intermediate with concomitant HCl elimination. The second and common step is the cleavage of the lactone ring with formation of CO and the corresponding aldehyde. In addition, some theoretical studies have been conducted with the aim of complementing the understanding of the molecular mechanisms associated with these decomposition processes.[6−10] The combination of experimental and theoretical results yields a precise idea of the nature for the molecular mechanisms associated with this reaction pathway.

In 1987, Chuchani and Rotinov studied the kinetics for the pyrolysis of 2-chloropropionic acid,[11] in which acetaldehyde, carbon monoxide, and hydrogen chloride were obtained. The mechanism was believed to proceed via a polar five-member cyclic TS as described in Scheme 1. This unusual HCl elimination led to a theoretical study of the 2-chloropropionic acid decomposition by using ab initio calculations at MP2/6-31G** level.[6] The theoretical result agrees with the experimental data describing a two-step mechanism involving the formation of the α-propiolactone intermediate. The first-step transition structure was associated with a five-member ring with participation of leaving chloride and hydrogen, assisted by the carbonyl oxygen of the COOH group, as shown in Scheme 1. In the second step, the unstable α-propiolactone intermediate decomposes to acetaldehyde and CO.

As an extension to the 3-substituted carboxylic acids, Chuchani et al. have studied the decomposition reaction of 3-chloropropionic acid.[4] However, it was found very difficult to make a complete kinetic work: the pyrolytic elimination just showed a first-order parallel decomposition at only one temperature (Scheme 2). Then, to procure a more reliable interpretation concerning the mechanistic elimination of the chloride leaving group at the position-3 of propionic acid, and avoid any possible parallel elimination, the present work aimed at examining the pyrolysis kinetics of 3-chloropivalic acid (3-chloro-2,2-dimethylpropionic acid), and we report a combination of kinetic experimental and theoretical studies of this decomposition process. The main objectives are to obtain the kinetic parameters and to characterize the stationary points on reactive PES in order to describe the nature of the molecular mechanism for the decomposition process.

The present paper is organized as follows: in Sections 2 and 3 the experimental details and the computational method and model are explained, respectively; in Section 4 the experimental and theoretical results are presented and discussed. Section 5 presents conclusions and closes the paper.

2. Experimental Section

3-Chloropivalic acid of 99.0% purity was bought from Aldrich. The pyrolysis product isobutene was analyzed by GLC, in a column of Porapak Q 80−100 mesh, while the HCl gas was quantitatively estimated by titration with a solution of 0.04

* Author to whom correspondence should be addressed.
[†] Instituto Venezolano de Investigaciones Científicas (I.V.I.C.).
[‡] Universitat Jaume I.
[§] Universitat de València.

10.1021/jp003560t CCC: $20.00
Published on Web 02/13/2001

SCHEME 1: 2-Chloropropionic Acid Pyrolysis Mechanisms

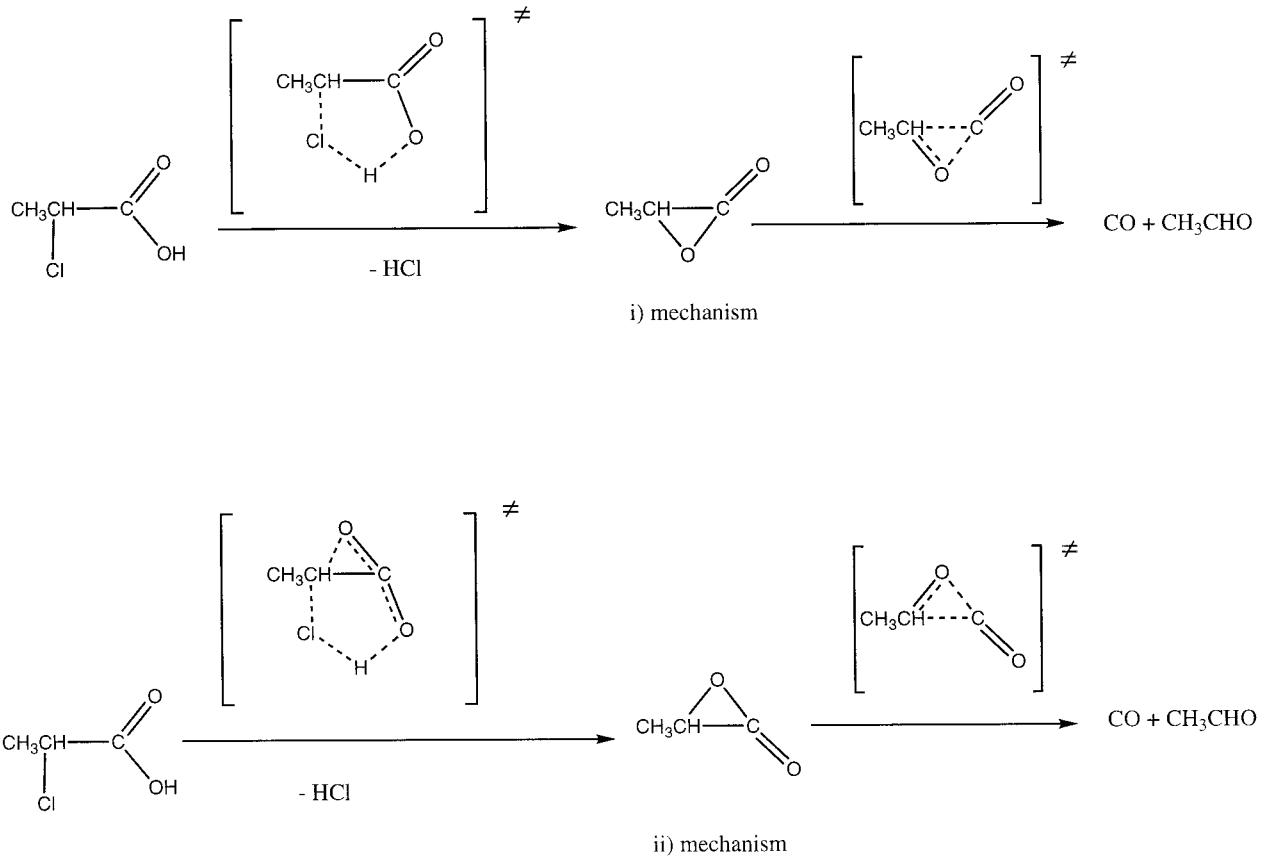

SCHEME 2: 3-Chloropropionic Acid Pyrolysis Mechanism

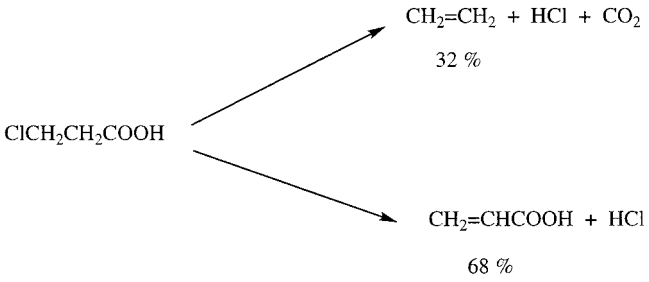

N NaOH. The identities of the substrate and product were additionally verified with a mass spectrometer and NMR spectroscopy.

The chloropivalic acid substrate was dissolved in a quantity of toluene at least equal to that of the substrate. The pyrolysis experiments were carried out in a static reaction apparatus as previously described,[12,13] but with some modifications and additions of modern electronic and electrical devices. The reaction vessels were seasoned with allyl bromide. The presence of toluene served as free radical suppresser. The concentration of the substrate is described as P_0 in pressure units of Torr. This P_0 is obtained by introducing 0.05−0.15 mL of the solution into the reaction vessel. These amounts, when applying the molar fraction correction, give pressures between 40 and 120 Torr. Consequently, tables describing P_0 are the initial concentration of the substrate in pressure units. The rate coefficients were determined by HCl titration. The temperature was controlled by a resistance thermometer controller type SHINKO DIC-PS 25TR maintained within ±0.2 °C and measured with a calibrated platinum−platinum-13% rhodium thermocouple. No temperature gradient was found along the reaction vessel. The substrate in toluene was injected directly into the reaction vessel with a syringe through a silicone rubber septum.

3. Computational Method and Model

The transition state theory (TST)[14,15] was devised to facilitate the interpretation of rate coefficients, and is used almost universally by chemists interested in reaction mechanisms.[16,17] We have selected this method to calculate the kinetic parameters in the present study.

Calculations at MP2 level of theory with the 6-31G** basis set[18] have been performed with the Gaussian98[19] program. The Berny analytical gradient optimization routines[20,21] were used for optimization. The requested convergence on the density matrix was 10^{-9} atomic units; the threshold value of maximum displacement was 0.0018 Å, and that of maximum force was 0.00045 hartree/bohr. The nature of each stationary point was established by calculating and diagonalizing the Hessian matrix (force constant matrix). The transition structures were characterized by means of a normal-mode analysis. The unique imaginary frequency associated with the transition vector (TV),[22] i.e., the eigenvector associated with the unique negative eigenvalue of the force constant matrix, has been characterized. The intrinsic reaction coordinate (IRC)[23] path was traced in order to check and obtain the energy profiles connecting each transition structure to the two associated minima of the proposed mechanism, by using the second-order González−Schlegel integration method.[24,25]

Each stationary point in the potential energy surface (PES) is characterized by an index which is equal to the number of negative eigenvalues of the Hessian matrix (0 for a minimum, 1 for a saddle point). This index is also the number of imaginary wavenumbers obtained in a normal-mode analysis of the corresponding molecular structure. This analysis also provides

TABLE 1: Ratio of Final to Initial Pressure (pressures in Torr)[a]

temperature (°C)	P_0	P_f	P_f/P_0	average
389.0	61.6	174	2.58	
399.5	71.7	180.7	2.52	
409.7	72.8	208.3	2.86	2.63
419.2	86.2	220.7	2.56	
430.1	75.8	200.9	2.65	

[a] Seasoned vessel and in the presence of toluene.

thermodynamic quantities such as zero-point vibrational energy (ZPVE), temperature corrections ($E(T)$) and the absolute entropy ($S(T)$),[26] and consequently the rate coefficient can be estimated. Temperature corrections and absolute entropies were obtained assuming ideal gas behavior, from the harmonic frequencies and moments of inertia by standard methods.[27] A temperature of 673.15 K (400 °C), inside the experimental range was taken in the calculations.

The first-order rate coefficient ($k(T)$) was computed using the TST [14,28] and assuming that the transmission coefficient is equal to 1, as expressed by the following relation:

$$k(T) = (kT/h)\exp(-\Delta G^{\ddagger}/RT) \quad (1)$$

where $\Delta G^{\ddagger}$ is the Gibbs free energy change between the reactant and its corresponding transition structure, and k and h are the Boltzmann and Planck constants, respectively. $\Delta G^{\ddagger}$ was calculated as follows:

$$\Delta G^{\ddagger} = \Delta H^{\ddagger} - T\Delta S^{\ddagger} \quad (2)$$

and

$$\Delta H^{\ddagger} = \mathrm{PEB} + \Delta\mathrm{ZPVE} + \Delta E(T) \quad (3)$$

where PEB is the potential energy barrier and $\Delta ZPVE$ and $\Delta E(T)$ are the differences of ZPVE and temperature corrections between the TS and the corresponding reactant, respectively. $\Delta S^{\ddagger}$ is obtained directly as the entropy (taken from the normal-mode Gaussian98 outputs) difference between the TS and its corresponding reactant.

4. Results and Discussion

4.1. Experimental Results. The products of the gas-phase decomposition of 3-chloropivalic acid, in a static system seasoned with allyl bromide and in the presence of the free-radical inhibitor toluene, are isobutene, HCl, and CO_2.

$$ClCH_2C(CH_3)_2COOH \rightarrow CH_2{=}C(CH_3)CH_3 + HCl + CO_2 \quad (4)$$

The stoichiometry (eq 4) required that, for very long reaction time, the final pressure, P_f, should be three times the initial reactant pressure, P_0. The average experimental P_f/P_0 value at five different temperatures and 10 half-lives was 2.63 (Table 1). The small departure from the theoretical stoichiometry was due to the little polymerization of isobutylene in the presence of HCl gas, as was checked by introducing a sample of isobutylene in the reaction vessel (and in the presence of HCl gas): a decrease of the olefin pressure is observed. In addition, a compound of relatively high molecular weight, containing only C and H, product of the isobutylene polymerization, was found by using our GC/MS. Verification of the above stoichiometry, up to 50% reaction, was possible by comparing the percentage decomposition of the substrate calculated from pressure measurements with the quantitative titration analysis of HCl with a solution 0.04 N of NaOH (Table 2).

TABLE 2: Stoichiometry of the Reaction at 419.2 °C[a]

time, min	2.5	5	8	10	15
reaction (%)(pressure)	19.4	30.1	40.0	45.5	51.8
HCl (%)(titration)	19.2	29.5	39.1	43.8	49.5

[a] Vessel seasoned with allyl bromide, in the presence of toluene inhibitor. The % reaction pressure is estimated by using equation $(P_T/P_0 - 1) \times 100$.

TABLE 3: Homogeneity of the Reaction at 419.2 °C

S/V (cm^{-1})[a]	10^4k_1 (s^{-1})[b]	10^4k_1 (s^{-1})[c]
1	1.21[d]	7.59
6	0.23[d]	7.49

[a] S = surface, V = volume. [b] Clean Pyrex vessel. [c] Seasoned vessel. [d] Several runs gave irregular k values.

TABLE 4: Effect of the Inhibitor Toluene on Rates at 419.2 °C

P_0	P_i	P_i/P_0	10^4k_1 (s^{-1})
70.8	47.7	0.7	8.01
86.7	151.5	1.8	7.34
65.5	177	2.7	7.59
74	219	3.0	7.40
43	219.5	6.2	7.65

Pressure of the substrate (torr, P_0), pressure of the inhibitor toluene (torr, P_i).

TABLE 5: Invariability of the Rate Coefficients with Initial Pressure at 419.2 °C

P_0 (Torr)	43	65.5	70	86.4	120.5
10^4k_1 (s^{-1})	7.65	7.59	7.64	7.34	7.50

The effect of the surface on the rate of decomposition was examined by carrying out several runs in a vessel with a surface-to-volume ratio of 6.0 cm^{-1} relative to that of the normal vessel equal to 1.0 cm^{-1}. The packed and unpacked Pyrex vessels, seasoned with allyl bromide, had no effect on rates. However, the packed and unpacked clean Pyrex vessels gave a small heterogeneous effect (Table 3).

The pyrolysis experiments were carried out in the presence of an amount of free radical suppresser toluene, at least equal to that of chloropivalic substrate, to prevent any possible chain reactions. The effect of different proportions of toluene in the decomposition process is shown in Table 4. No induction period was observed. The rate coefficients were reproducible with a relative standard deviation not greater than 5% at a given temperature.

The first-order rate coefficients of this chloroacid, calculated from $k_1 = (2.303/t)\log[2P_o/(3P_o - P_t)]$, were independent of its initial pressure (Table 5). Plotting $\log(3P_o - P_t)$ against time t gave a good straight line up to 50% decomposition (Figure 1). The approximate straight line is an indication of a first-order reaction. The temperature dependence of the rate coefficients and the corresponding Arrhenius equation are described in Table 6 (90% confidence coefficient from least-squares procedure).

The replacement of the two hydrogens at carbon-2 of 3-chloropropionic acid by methyl groups, ***i.e.***, 3-chloropivalic acid, shows a significant decrease in the rate of decomposition (Table 7). This result may infer that pathways different from those of the 2-, 4-, and 5-chlorocarboxylic acids[4,11] pyrolysis may occur. Consequently, to establish the most adequate mechanisms of the 3-chloroacids elimination processes, a theoretical study has been conducted.

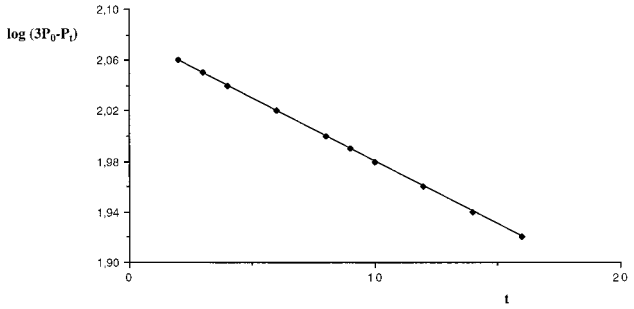

Figure 1. Plot of $\log(3P_0 - P_t)$ against t (min) at $T = 409.7$ °C. P_0 and P_t are given in Torr. $r = 0.9999$.

TABLE 6: Variation of Rate Coefficients with Temperature

T (°C)	380.5	389.0	399.5	409.7	419.2	430.1
$10^4 k_1$ (s^{-1})	0.93	1.51	2.74	4.93	7.59	13.42

$$\log k_1\,(s^{-1}) = (12.42 \pm 0.36) - (205.8 \pm 4.7)\ \text{kJ mol}^{-1}\ (2.303RT)^{-1}$$

TABLE 7: Comparative Rate Coefficients (k_1, s^{-1}) at 340.0 °C, and Relative Rate of Olefin Formation[a]

substrate	$10^5 k_1$	relative rate olefin formation
$ClCH_2CH_2COOH$	14.7	16.3 $CH_2{=}CH_2$
$ClCH_2C(CH_3)_2COOH$	0.90	1.0 $CH_2{=}C(CH_3)_2$

[a] Data for 3-chloropivalic acid from ref 4.

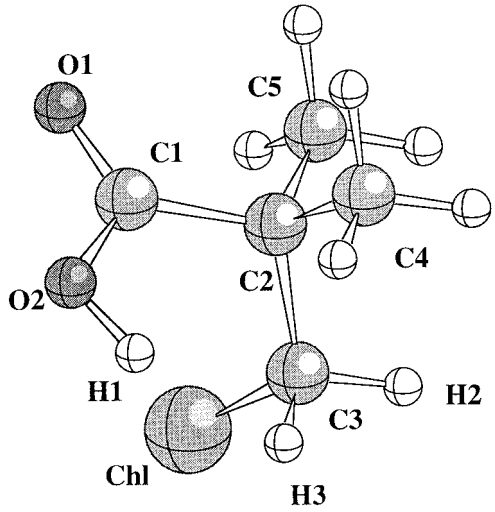

Figure 2. Optimized geometry of 3-chloropivalic acid, including atom numbering.

4.2. Theoretical Results. The equilibrium geometry of 3-chloropivalic acid is depicted in Figure 2, including atom numbering. An exhaustive exploration of PES related with the decomposition of this system renders two TSs (see Figure 4): **TS1** is associated with the decomposition process, and the TV is mainly controlled by the simultaneous C3−Chl, O2−H1 and C1−C2 breaking bonds, yielding directly the products in one step. Another TS, corresponding to the butyrolactone formation with HCl elimination (**TS2**) has also been found with a large value of relative energy (see Table 9).

4.2.1. Energetics and the Kinetic Parameters. The thermochemical data of products relative to the reactants, (ΔH, ΔS, and ΔG) obtained from the normal mode Gaussian98 outputs, as explained, are reported in Table 8. The activation parameters ($\Delta H^{\ddagger}$, $\Delta S^{\ddagger}$, $\Delta G^{\ddagger}$) together with the calculated elementary first-order rate constants, corresponding to the decomposition reaction of the 3-chloropivalic acid through **TS1** and **TS2**, and experimental values of k_1 are reported in Table 9. It can be seen that the decomposition process occurs through **TS1** rather than through **TS2**: **TS1** is ca. 90 kJ mol^{-1} more stable.

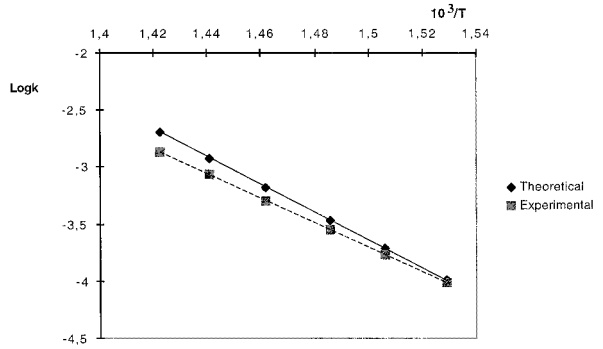

Figure 3. Arrhenius plots obtained from experimental and theoretical data. Log k (s^{-1}) versus $10^3/T$ (K^{-1}). The experimental value of log A is 12.42 ± 0.36 s^{-1}, while the theoretical value is 13.71 s^{-1}. The experimental value of activation energy is 205.8 ± 4.7 kJ·mol^{-1}, while the theoretical value is 227.1 kJ·mol^{-1}.

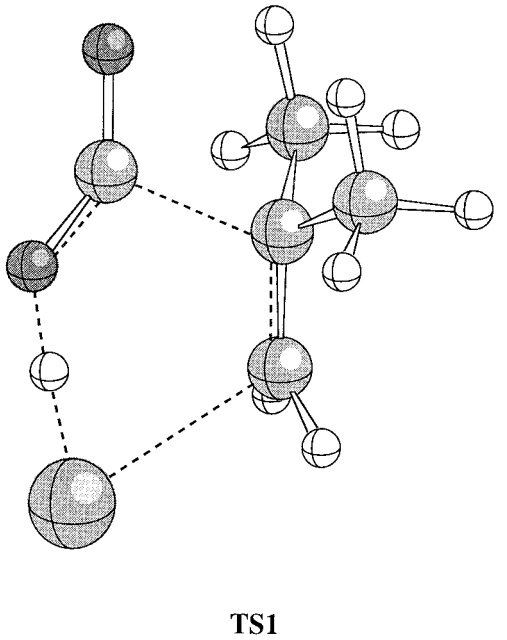

TS1

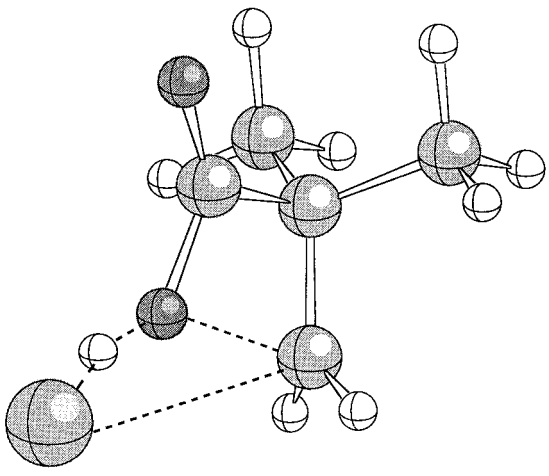

TS2

Figure 4. Optimized geometries of the **TS1** and **TS2**.

TABLE 8: Relative Enthalpies (ΔH, kJ mol^{-1}), Entropies (ΔS, J mol^{-1} K^{-1}) and Gibbs Free Energies (ΔG, kJ mol^{-1})

	ΔH	ΔS	ΔG
products	−13.45	333.12	−237.69

TABLE 9: Activation Enthalpies ($\Delta H^{\ddagger}$, kJ mol^{-1}), Entropies ($\Delta S^{\ddagger}$, J mol^{-1} K^{-1}) and Gibbs Free Energies ($\Delta G^{\ddagger}$, kJ mol^{-1})[a]

	$\Delta H^{\ddagger}$	$\Delta S^{\ddagger}$	$\Delta G^{\ddagger}$	k
TS1	221.5	10.92	214.15	3.4×10^{-4}
TS2	304.68	−0.47	305.01	3.0×10^{-11}

[a] Theoretically calculated (at 673.15 K) first-order rate coefficients (k, s^{-1}). The interval (calculated taking into account the experimental uncertainties) for the observed rate coefficient at 673.15 K is from 5.357×10^{-5} to 1.507×10^{-3} s^{-1}.

The decomposition of chloropivalic acid is an exothermic process; the ΔH value is negative. The global process is spontaneous, the ΔG value is −237.69 kJ mol^{-1}.

An analysis of the experimental and theoretical values of $\Delta H^{\ddagger}$ and $\Delta S^{\ddagger}$ for **TS1**, show discrepancies, mainly regarding $\Delta S^{\ddagger}$. However, a comparison between the values for the calculated and experimental k_1 rate constant shows a good agreement. The experimental interval for the observed rate coefficient at 673.15 K is 5.357×10^{-5} to 1.507×10^{-3} s^{-1}. The theoretical value falls into the experimental range.

In Figure 3, the experimental and theoretical Arrhenius plots are presented. It can be seen that, although the rate constants agree, some divergences were found between the theoretical and experimental values for the A-factors and the slope (activation energy) of both experimental and theoretical Arrhenius plots. Probably, the use of more sophisticated treatments of internal rotors and tunneling or the use of more demanding quantum mechanical calculations (a large basis set representation, higher calculation level) could improve the theoretical results.

4.2.2. Geometries and Transition Vectors. TVs and geometries for the transition structure corresponding to the decomposition process (**TS1**) and for **TS2** are reported in Table 10. These stationary points are depicted in Figure 4. Further information on TSs (the whole set of geometric parameters, the force constants, all positive eigenvalues, or all vibrational frequencies) is available from the authors on request (andres@exp.uji.es; safont@exp.uji.es).

For **TS1** (see Table 10), the main component of TV is the H1−O2 distance, in phase with the C1−C2 and C3−Chl distances. These components correspond to the decomposition process. In addition, the O1−C1−C2 and O2−C1−C2 bond angles in antiphase with the aforementioned distances components have also a significant participation in the TV; the opening of the CO_2 angle and the elimination process are coupled. The C2−C3 and C1−O2 motions slightly participate in the TV: the C2−C3 and C1−O2 bonds are somewhat shortened while the elimination process takes place, because they evolve from single to double bonds.

The geometric parameters of **TS1** displayed in Table 10 correspond with a concerted molecular mechanism: the elimination processes appear to be roughly simultaneous. Thus, the distances for the breaking bonds C3−Chl, H1−O2, and C1−C2 are 2.45, 1.16, and 1.98 Å, respectively, while the H1−Chl forming bond distance (data not shown in Table 10) is 1.53 Å. The distances for the bonds that evolve from single to double, C2−C3 and C1−O2, are 1.39 and 1.26 Å, respectively. The simultaneous character can be better shown by an analysis of the bond order evolution and the synchronicity values (see below).

TABLE 10: Imaginary Frequency (Freq, cm^{-1}), Hessian Unique Negative Eigenvalue (Eig, a. u.), Main Components of the Transition Vector (C, a. u.), and Corresponding Geometric Parameters (G, bonds in Å, Bond and Dihedral Angles in Degrees) for the TS1 and TS2

	TS1	
Freq	1166.46i	
Eig	−0.15055	
	C	G
C1−C2	0.443	1.978
C2−C3	−0.135	1.392
C3−Chl	0.425	2.451
C1−O2	−0.161	1.255
H1−O2	0.644	1.159
O1−C1−C2	−0.220	107.72
O2−C1−C2	−0.141	114.01
H1−O2−C1	0.127	115.35
C5−C2−C4−C3	−0.153	−137.77
H3−C3−C2−C1	0.134	−97.98
	TS2	
Freq	796.82i	
Eig	−0.98053	
	C	G
C1−C2	0.206	1.528
C3−Chl	−0.197	2.746
H1−O2	−0.338	1.068
C4−C2−C3	−0.260	109.98
C1−C2−C4	−0.268	108.44
O1−C1−C2	−0.184	127.49
O2−C1−C2	0.460	106.49
C1−C2−C4−C3	0.522	106.81
H2−C3−C2−C1	0.156	126.87
H3−C3−C2−C1	0.212	−71.77
O2−C1−C2−C3	0.179	−4.48
Chl-C3−C2−C1	−0.115	65.02
H1−O2−C1−C2	0.116	−70.70

For **TS2** (see Table 10), the bond distances that participate significantly in the TV are the H1−O2 and C3−Chl breaking bonds, in antiphase with the C1−C2 distance. However, the main components of the TV correspond to a bond and a dihedral angle (O2−C1−C2 and C1−C2−C4−C3, respectively). These components are related with the closure of the lactone. This reaction pathway corresponds to the ring closure of the lactone with formation of HCl. An analysis of the geometric parameters values shows an asynchronous character for this TS. The C3−Chl bond distance is 2.75 Å, larger than the preceding case. The H1−O2 bond distance is 1.07 Å, and the O2−C3 distance (data not shown in Table 10) is 2.15 Å.

These data seem to indicate that the carbon−chloride bond is polarized before the leaving of the hydrogen and the closure of the lactone ring. Again, an analysis of the bond order evolution and synchronicity value will shed more light on this issue (see below).

The imaginary frequency values are 1166i cm^{-1} for **TS1** and 796i for **TS2**; indicating that these stationary points are associated with the heavy atoms motions, mainly **TS2**.

4.2.3. Bond Order Analysis. To obtain a deeper analysis of the extent of bond or bond forming/breaking along the reaction pathway, the bond order (B) concept has been used.[29−31] The Wiberg bond indices [32] have been computed by using the Natural Bond Orbital (NBO) [33,34] analysis as implemented in Gaussi-

TABLE 11: Wiberg Bond Indices (B_i), and Percentage of Evolution through the Chemical Process (%Ev) of the Bond Indices at the TS1 and TS2 Calculated by Means of Eq 8[a]

		C1−C2	C2−C3	C3−Chl	Chl−H1	H1−O2	C1−O2
TS1	B_i^R	0.950	0.985	1.012	0.000	0.728	0.978
	B_i^{TS}	0.525	1.320	0.312	0.438	0.342	1.302
	%Ev	44.7	35.3	69.2	47.5	53.0	38.2
	Sy			0.89			

		O2−C3	C3−Chl	Chl-H1	H1−O2
TS2	B_i^R	0.002	1.012	0.000	0.728
	B_i^{TS}	0.183	0.164	0.290	0.440
	%Ev	21.2	83.8	31.5	39.6
	Sy		0.70		

[a] The synchronicity value (Sy) obtained from eq 5 is also included.

an98.[19] Several breaking/forming bond processes are involved in the fragmentation, and the global nature of the decomposition reaction can be monitored by means of the synchronicity (Sy) concept proposed by Moyano et al.,[35] using the following expression:

$$Sy = 1 - \frac{\sum_{i=1}^{n} \frac{|\delta B_i - \delta B_{av}|}{\delta B_{av}}}{2n - 2} \quad (5)$$

In eq 5, n is the number of bonds directly involved in the reaction, and the relative variation of the bond index is obtained from

$$\delta B_i = \frac{B_i^{TS} - B_i^{R}}{B_i^{P} - B_i^{R}} \quad (6)$$

where the superscripts *TS*, *R*, and *P* refer to the TS, reactant, and product, respectively. The average value is therefore

$$\delta B_{av} = n^{-1} \sum_{i=1}^{n} \delta B_i \quad (7)$$

Synchronicities calculated from expression 5 and the Wiberg bond indices [32] of the breaking/making bond processes are reported in Table 11. The percentage of evolution of the bond order through the chemical step has been calculated by using

$$\% \text{ Ev} = \delta B_i \times 100 \quad (8)$$

The results are also included in Table 11. For **TS1,** it can be seen that all the percentages of evolution of the bond order are within a range of 35% to 69%, thus describing a highly synchronous TS. The displacement of the chloride atom is the more advanced motion (69.2% evolution), while the C2−C3 and C1−O2 bonds, that evolve from single to double bonds, are late, displaying a small evolution percentage. Then, the extension of the C3−Chl bond with initial migration of the chloride atom can be seen as the driving force for the decomposition process. The synchronicity value of 0.89 shows that the reaction pathway can be described as concerted and highly synchronous.

TS2 has a larger asynchronous character than **TS1**; the corresponding Sy value is 0.70. The O2−C3 and the Chl−H1 forming bond processes are late, 21% and 31.5% evolution, respectively, while the C3−Chl is very advanced, 84% evolution.

An analysis of the NBO charges at reactant shows a large positive charge at C1 (1.01) and at H1 (0.53). Negative charges appear at C2 (−0.18), C3 (−0.40), C4 (−0.65), C5 (−0.65), O1 (−0.71), O2 (−0.80), and Chl (−0.10) centers. At **TS1**, the charge at C1 has slightly increased to 1.16, while the charge on H1 has slightly decreased to 0.46. On C2, an important increase of the positive charge, up to 0.33, takes place, and on C3, a decrease of negative charge, down to −0.03, is sensed. The negative charges at C4 and C5 are the same (−0.65), and a slight decrease of negative charges on the two oxygens can be sensed, down to −0.66 and −0.77 for O1 and O2, respectively. The chlorine atom supports now a negative charge larger than before (−0.47). Then, from an electronic point of view, the negative charge mainly moves from C2 and C3 to Chl. This also indicates that the extension and polarization of the C3−Chl bond can be seen as the driving force for the decomposition process.

5. Conclusions

This work can be considered a collaborative project between experimental and theoretical research groups. The 2-chloropivalic acid has been pyrolyzed, and the corresponding rate coefficient has been determined by HCl titration. The kinetic parameters and the reactive potential energy surface, at MP2/6-31G** calculation level, have been theoretically obtained. The first-order rate coefficient was then evaluated in terms of transition state theory and the theoretical results have been compared with the experimental data. From the combination of experimental and theoretical studies, the following conclusions can be drawn:

(1) The experimental data show that the decomposition is homogeneous, unimolecular, and follows a first-order rate law, which has been determined.

(2) The decomposition process, via a six-member cyclic transition structure, **TS1**, yields the corresponding products in one step. The molecular mechanism can be described as concerted and highly synchronous.

(3) An analysis of bond orders and NBO charges suggests that the extension and polarization of the C3−Chl bond with initial migration of the chlorine atom seems to be the driving force for the decomposition process at **TS1**.

(4) An alternative **TS2**, associated with a reaction pathway including butyrolactone formation, has also been found, although its high energy makes it kinetically irrelevant.

(5) An analysis and comparison of the calculated and experimental kinetic parameters and Arrhenius plots point out the validity of the theoretical approaches. A good agreement is achieved between the theoretical and experimental results.

Acknowledgment. This work was supported by research funds of the Ministerio de Educación y Ciencia of the Spanish Government by DGICYT (project PB96-0795-C02-02) and of CONICIT (Consejo Nacional de Investigaciones Científicas y Tecnológicas) of Venezuela (project S1-97000005). All calculations were performed on two Silicon Graphics Power Challenge L of the Servei d'Informàtica of the Universitat Jaume I. We are most indebted to this center for providing us with computer capabilities.

References and Notes

(1) Chuchani, G.; Rotinov, A. *Int. J. Chem. Kinet.* **1989**, *21*, 367.
(2) Chuchani, G.; Domínguez, R. M.; Rotinov, A. *Int. J. Chem. Kinet.* **1991**, *23*, 779.
(3) Chuchani, G.; Martín, I.; Rotinov, A.; Domínguez, R. M. *J. Phys. Org. Chem.* **1993**, *6*, 54.

(4) Chuchani, G.; Martín, I.; Rotinov, A.; Domínguez, R. M.; Pérez I. M. *J. Phys. Org. Chem.* **1995**, *8*, 133.
(5) Chuchani, G.; Domínguez, R. M. *Int. J. Chem. Kinet.* **1995**, *27*, 85.
(6) Safont, V. S.; Moliner, V.; Andrés, J.; Domingo, L. R. *J. Phys. Chem.* **1997**, *101*, 1859.
(7) Domingo, L. R.; Andrés, J.; Moliner, V.; Safont, V. S. *J. Am. Chem. Soc.* **1997**, *119*, 6415.
(8) Domingo, L. R.; Picher, M. T.; Andrés, J.; Safont, V. S.; Chuchani, G. *Chem. Phys. Lett.* **1997**, *274*, 422.
(9) Domingo, L. R.; Picher, M. T.; Safont, V. S.; Andrés, J.; Chuchani, G. *J. Phys. Chem.* **1999**, *103*, 3935.
(10) Rotinov, A.; Chuchani, G.; Andrés, J.; Domingo, L. R.; Safont, V. S. *Chem. Phys.* **1999**, *246*, 1.
(11) Chuchani, G.; Rotinov, A. *Int. J. Chem. Kinet.* **1987**, *19*, 789.
(12) Swinbourne, E. S. *Aust. J. Chem.* **1958**, *11*, 334.
(13) Maccoll, A. *J. Chem. Soc.* **1965**, 965.
(14) Glasstone, K. J.; Laidler, K. J.; Eyring, H. *The Theory of Rate Processes*; McGraw-Hill: New York, 1941.
(15) Laidler, K. J. *Theories of Chemical Reaction Rates*; McGraw-Hill: New York, 1969.
(16) Petersson, G. A. *Theor. Chem. Acc.* **2000**, *103*, 190.
(17) Garrett, B. C. *Theor. Chem. Acc.* **2000**, *103*, 200.
(18) Frisch, M. J.; Pople, J. A.; Binkley, J. S. *J. Chem. Phys.* **1984**, *80*, 3265.
(19) Frisch, M. J.; Trucks, G. W.; Schlegel, H. B.; Scuseria, G. E.; Robb, M. A.; Cheeseman, J. R.; Zakrzewski, V. G.; Montgomery, J. A., Jr.; Stratmann, R. E.; Burant, J. C.; Dapprich, S.; Millam, J. M.; Daniels, A. D.; Kudin, K. N.; Strain, M. C.; Farkas, O.; Tomasi, J.; Barone, V.; Cossi, M.; Cammi, R.; Mennucci, B.; Pomelli, C.; Adamo, C.; Clifford, S.; Ochterski, J.; Petersson, G. A.; Ayala, P. Y.; Cui, Q.; Morokuma, K.; Malick, D. K.; Rabuck, A. D.; Raghavachari, K.; Foresman, J. B.; Cioslowski, J.; Ortiz, J. V.; Baboul, A. G.; Stefanov, B. B.; Liu, G.; Liashenko, A.; Piskorz, P.; Komaromi, I.; Gomperts, R.; Martin, R. L.; Fox, D. J.; Keith, T.; Al-Laham, M. A.; Peng, C. Y.; Nanayakkara, A.; Gonzalez, C.; Challacombe, M.; Gill, P. M. W.; Johnson, B.; Chen, W.; Wong, M. W.; Andres, J. L.; Gonzalez, C.; Head-Gordon, M.; Replogle, E. S.; Pople, J. A. Gaussian98; Gaussian, Inc.: Pittsburgh, PA, 1998.
(20) Schlegel, H. B. *J. Comput. Chem.* **1982**, *3*, 214.
(21) Schlegel, H. B. *J. Chem. Phys.* **1982**, *77*, 3676.
(22) McIver, J. W., Jr. *Acc. Chem. Res.* **1974**, *7*, 72.
(23) Fukui, K. *J. Phys. Chem.* **1970**, *74*, 4161.
(24) González, C.; Schlegel, H. B. *J. Phys. Chem.* **1990**, *94*, 5523.
(25) González, C.; Schlegel, H. B. *J. Chem. Phys.* **1991**, *95*, 5853.
(26) Hehre, W. J.; Radom, L.; Schleyer, P. v. R.; Pople, J. A. *Ab Initio Molecular Orbital Theory*; John Wiley & Sons: New York, 1986.
(27) McQuarrie, D. *Statistical Mechanics*; Harper & Row: New York, 1986.
(28) Benson, S. W. *The foundations of chemical kinetics*; McGraw-Hill: New York, 1960.
(29) Varandas, A. J. C.; Formosinho, S. J. F. *J. Chem. Soc., Faraday Trans. 2* **1986**, 282.
(30) Lendvay, G. *J. Mol. Struct. THEOCHEM* **1988**, *167*, 331.
(31) Lendvay, G. *J. Phys. Chem.* **1989**, *93*, 4422.
(32) Wiberg, K. B. *Tetrahedron* **1968**, *24*, 1083.
(33) Reed, A. E.; Curtiss, L. A.; Weinhold, F. *Chem. Rev.* **1988**, *88*, 899.
(34) Reed, A. E.; Weinstock, R. B.; Weinhold, F. J. *J. Chem. Phys.* **1985**, *83*, 735.
(35) Moyano, A.; Pericàs, M. A.; Valentí, A. *J. Org. Chem.* **1989**, *54*, 573.